Acta Cryst. (1994). D**50**, 859–868

Stuctures of Human and Porcine Aldehyde Reductase: an Enzyme Implicated in Diabetic Complications

BY OSSAMA EL-KABBANI

The University of Alabama at Birmingham, Center for Macromolecular Crystallography, Birmingham, Alabama 35294-0005, *USA*

NANCY C. GREEN

Queen's University, Department of Biochemistry, Kingston, Ontario K7L 3N6, Canada

GUANGDA LIN, MIKE CARSON, STHANAM V. L. NARAYANA AND KAREN M. MOORE

The University of Alabama at Birmingham, Center for Macromolecular Crystallography, Birmingham, Alabama 35294-0005, *USA*

T. GEOFFREY FLYNN

Queen's University, Department of Biochemistry, Kingston, Ontario K7L 3N6, Canada

AND LAWRENCE J. DELUCAS

The University of Alabama at Birmingham, Center for Macromolecular Crystallography, Birmingham, Alabama 35294-0005, *USA*

(*Received* 15 *January* 1994; *accepted* 16 *May* 1994)

Abstract

The crystal structures of porcine and human aldehyde reductase, an enzyme implicated in complications of diabetes, have been determined by X-ray diffraction methods. The crystallographic *R* factor for the refined porcine aldehyde reductase model is 0.19 at 2.8 Å resolution. There are two molecules in the asymmetric unit related by a local non-crystallographic twofold axis. The human aldehyde reductase model has been refined to an *R* factor of 0.21 at 2.48 Å resolution. The amino-acid sequence of porcine aldehyde reductase revealed a remarkable homology with human aldehyde reductase. The coenzyme-binding site residues are conserved and adopt similar conformations in human and porcine aldehyde reductase apo-enzymes. The tertiary structures of aldhyde reductase and aldose reductase are similar and consist of a β/α-barrel, with the coenzyme-binding site located at the carboxy-terminus end of the strands of the barrel. The crystal structure of porcine and human aldehyde reductase should allow *in vitro* mutagenesis to elucidate the mechanism of action for this enzyme and facilitate the effective design of specific inhibitors.

Introduction

Aldehyde reductase (ALR1; EC 1.1.1.2)* is a monomeric enzyme that catalyzes the NADPH-dependent reduction of a wide range of aromatic and aliphatic aldehydes to their corresponding alcohols (Flynn, 1982). There is considerable pharmacological interest in aldehyde reductase and aldose reductase (ALR2: E.C. 1.1.1.21) as target enzymes for drugs used in the treatment of diabetic complications such as nephropathy, neuropathy and retinopathy (Kinoshita & Nishimura, 1988). Based on the metabolism of excess glucose *via* aldose and aldehyde reductase, the osmotic stress mechanism has been suggested to explain how tissue damage might be caused by glucose in diabetes (Kinoshita, 1974). While this metabolic pathway appears to be virtually dormant under normal physiological conditions, the hyperglycemia-induced increase in the flux of glucose

* The abbreviations used are: ALR1, aldehyde reductase; ALR2, aldose reductase; hALR1, human aldehyde reductase; pALR1, porcine aldehyde reductase; hALR2, human aldose reductase; pALR2, porcine aldose reductase; ADPRP, 2′-monophosphoadenosine-5′-diphosphoribose; PCR, polymerase chain reaction.

results in a correspondingly high rate of sorbitol production and NADPH and NADH consumption by aldose and aldehyde reductase (Gonzalez, Barnett, Aguayo, Chen & Chylack, 1984). This initiates a series of biochemical changes that result in cellular loss of functional integrity (Kinoshita, 1974).

Aldose reductase inhibitors are reported to: (1) Delay or prevent the onset of sugar cataracts in diabetic and galactosemic rats (Kador & Kinoshita, 1984). (2) Reverse delayed re-epithelization of denuded corneas in diabetic rats and humans (Kinoshita *et al.*, 1984). (3) Reverse decreased axonal transport and improve nerve conduction velocity in diabetic rats and humans (Tomlinson & Mayer, 1984; Ward, 1985; Boulton, 1986; Ryder, 1986). (4) Symptomatically improve painful diabetic neuropathy (Ward, 1985; Boulton, 1986). (5) Prevent retinal capillary basement-membrane thickening in galactosemic and diabetic fructose-fed rats (Frank, Keirn, Kennedy & Frank, 1983; Robinson, Kador & Kinoshita, 1983; Kojima *et al.* 1985; Shanks, D'Amico & Gragoudas, 1985; Dvornik, Millen & Kemper, 1986; Robinson *et al.*, 1986). (6) Ameliorate limited joint mobility in diabetic patients (Eaton, Sibbitt & Harsh, 1985). (7) Improve increased vascular permeability in diabetic and galactosemic rats (Williamson *et al.*, 1985).

There are no reported inhibitors of aldehyde reductase. It has been shown by biochemical studies that many aldose reductase inhibitors will also inhibit aldehyde reductase (Srivastava, Petrash, Sadana, Ansari & Partridge, 1982). Unfortunately, undesirable side effects (Spielberg *et al.*, 1991) or lack of efficacy (Srivastava *et al.*, 1982) have prevented clinical use of many of the currently available aldose reductase inhibitors. In order to develop potent and more specific inhibitors for aldose and aldehyde red-

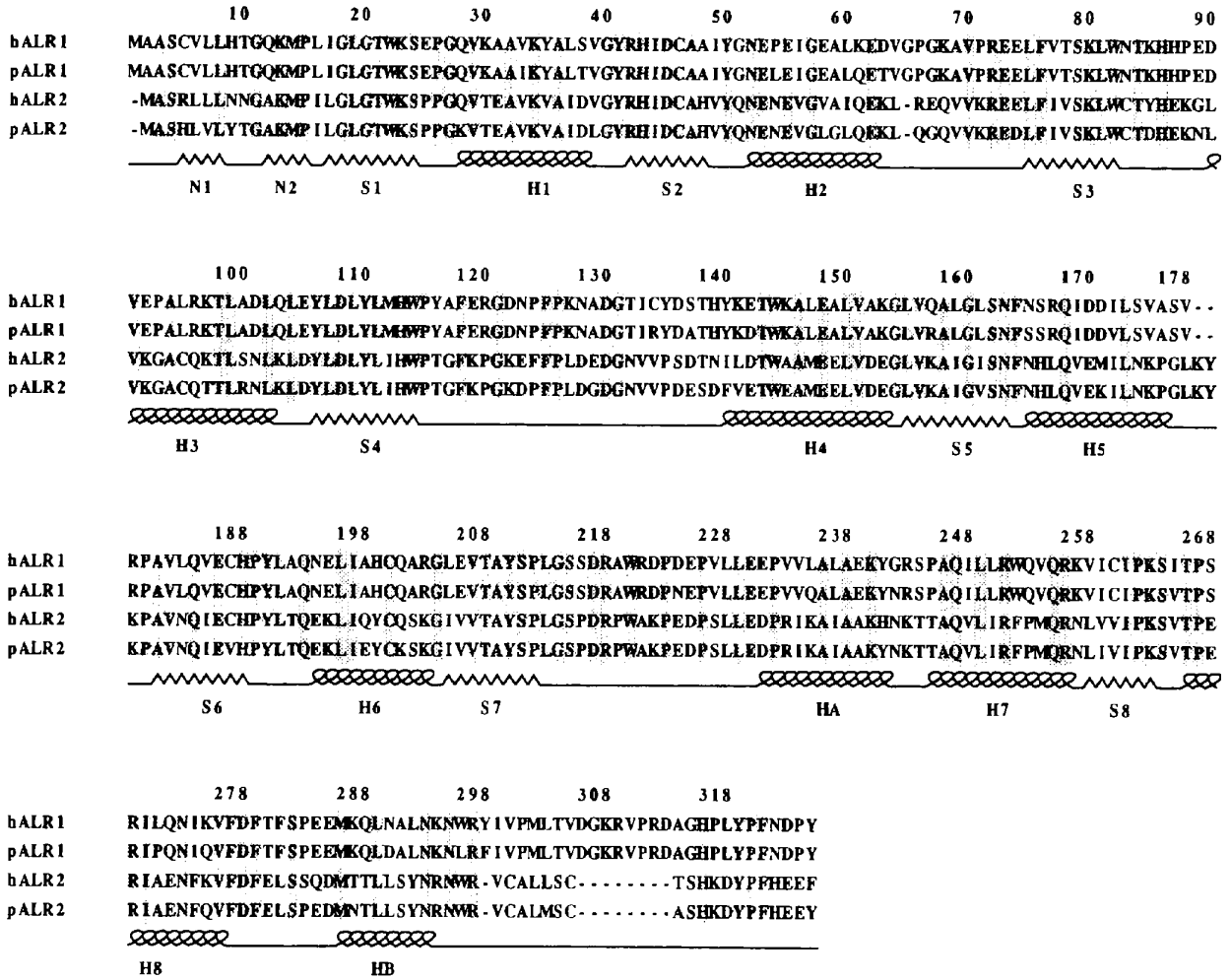

Fig. 1. Amino-acid sequences of human aldehyde reductase (hALR1), porcine aldehyde reductase (pALR1), human aldose reductase (hALR2) and porcine aldose reductase (pALR2). Secondary-structure assignments based on the hALR1 and pALR1 structures are noted below the residues. α-helices are designated as H, β-strands as S and strands of the N-terminal β-sheet as N. Residues that exhibit sequence identity are shaded.

uctase, attention has been turned to the possibilities of rational drug design based on the three-dimensional structures of these two enzymes and their mechanisms of action.

A preliminary structure determination of porcine aldose reductase (pALR2) has been reported (El-Kabbani *et al.*, 1991), as has the structure of porcine aldose reductase complexed with the coenzyme analog 2′-monophosphoadenosine-5′-diphosphoribose (ADPRP) (Rondeau *et al.*, 1992). The structure of human aldose reductase (hALR2) complexed with NADPH has been independently reported by two laboratories (Borhani, Harter & Petrash, 1992; Wilson, Bohren, Gabbay & Quiocho, 1992). In this study, we report the first crystallographic three-dimensional structures of aldehyde reductase (ALR1) isolated from porcine and human kidney.* The details of the crytallization and preliminary structure determination of porcine aldehyde reductase were reported earlier (El-Kabbani *et al.*, 1993).

Materials and methods

Purification and crystallization

Porcine kidney and human kidney aldehyde reductase were isolated and purified using a modification of the method of Cromlish & Flynn (1983). The two critical modifications to the published method were: (1) Use of a TRIS buffer system instead of sodium phosphate. (2) Inclusion of size-exclusion high-performance liquid chromatography as the final purification step. Monoclinic crystals of the porcine enzyme were grown by vapor diffusion from buffered ammonium sulfate solutions at pH 6.5 (El-Kabbani *et al.*, 1993). Orthorhombic crystals of human aldehyde reductase were grown at 293 K by vapor diffusion using the hanging-drop method (McPherson, 1985). 18 μl of protein (7 mg ml^{-1}), previously dialized against 10 m*M* PIPES buffer with 2 m*M* 2-mercaptoethanol and 10 m*M* β-octylglucoside, pH 6.2, were mixed with 9 μl 20% ammonium sulfate solution in 10 m*M* PIPES buffer, 2 m*M* 2-mercaptoethanol, 20 m*M* β-octylglucoside, pH 6.4. The droplets were vapor equilibrated against 1 ml of 35% ammonium sulfate solution in 50 m*M* PIPES buffer, 2 m*M* 2-mercaptoethanol, 20 m*M* β-octylglucoside, pH 6.4.

* Atomic coordinates and structure factors have been deposited with the Protein Data Bank, Brookhaven National Laboratory (Reference: 1ALR, R1ALRSF). Free copies may be obtained through The Managing Editor, International Union of Crystallography, 5 Abbey Square, Chester CH1 2HU, England. (Reference: GR368). At the request of the authors, the atomic coordinates will remain privileged until 1 November 1995 and the structure factors will remain privileged until 1 November 1998.

Amino-acid sequence determination

To assist in the refinement of the crystal structure of the enzyme, the cDNA of pig brain aldehyde reductase was cloned and the derived amino-acid sequence determined. Polymerase chain reaction (PCR) (Siaki *et al.*, 1985) using oligonucleotides (Core Facility at Queen's University) specific for human aldehyde reductase but not for aldose reductase was used to amplify a probe from human genomic DNA. The probe was nick translated following manufacturer's protocols (BRL) and used to screen a pig brain cDNA library (Clonetech) following the methods outlined in Sambrook, Fritsch & Maniatis (1990). One clone selected for sequencing was subcloned into the EcoRI site of pGEM3Zf+ (Promega). The insert was sequenced on both strands using successive oligonucleotide primers and a dideoxy DNA-sequencing kit (Pharmacia) following manufacturer's protocols. Full details of the cloning and sequencing will be published elsewhere.

Data collection

X-ray diffraction data from porcine aldehyde reductase crystals were recorded on a Siemens multiwire area detector and processed by the *Xengen* program package (Howard *et al.*, 1987). The space group is $P2_1$ with $a = 56.2$, $b = 98.1$, $c = 73.2$ Å and $\beta = 112.5°$. Final native data for porcine aldehyde reductase had 15830 out of 18032 possible unique reflections with 12090 reflections measured more than once at 2.8 Å resolution. The overall ratio of I to $\sigma(I)$ and the R(sym) on intensities equalled 17.1 and 10.7%, respectively (El-Kabbani *et al.*, 1993). R(sym) is defined as $\sum_{hkl}\sum_i^N|\bar{I} - I|/\sum_{hkl}N\bar{I}$, where $\bar{I}$ is the mean intensity of the N reflections with intensities I_i and common indices h, k and l.

Human aldehyde reductase crystals diffract to 2.46 Å resolution in Cu $K\alpha$ radiation (40 kV, 100 mA) generated by a fine-focus rotating anode generator (RU-200, Rigaku) and are stable for more than 100 h in the X-ray beam. The space group is $P2_12_12_1$, with $a = 82.6$, $b = 60.0$, $c = 66.2$ Å, $\alpha = \beta = \gamma = 90.0°$. X-ray diffraction data were recorded from one native crystal by using the procedure described above. The final native data had 11444 out of 12473 possible unique reflections with 11235 reflections measured more than once (resolution 2.46 Å). The R(sym) is equal to 8.3% and the overall mean ratio of I to $\sigma(I)$ equalled 37.1. The value of V_m is 2.16 Å Da^{-1} and the solvent content is 43%. There is one molecule in the asymmetric unit.

Structure determination

A preliminary structure of porcine aldehyde reductase was obtained by using a combination of molecu-

lar replacement and single isomorphous replacement techniques (El-Kabbani *et al.*, 1993). Atomic coordinates of porcine aldose reductase and a consensus primary sequence built by using human aldehyde reductase and porcine aldose reductase sequences were used as the starting model for molecular-replacement studies (the primary sequence for pALR1 was not available at this stage). The initial R factor equalled 0.43 at 2.8 Å resolution and dropped to 0.40 after rigid-body refinement, where R factor = $\Sigma|F_o - F_c|/\Sigma|F_o|$, F_o is the observed and F_c is the calculated structure factor. Side chains of amino-acid residues that were not included in the search model were fitted into the density using the human aldehyde reductase sequence (Bohren, Bullock, Wermuth & Gabbay, 1989) and *FRODO* software (Jones, 1978). After one round of model refitting and simulated-annealing refinement using the slow-cooling protocol of the *X-PLOR* package (Brünger, Krukowski & Erickson, 1990) followed by 40 energy-minimization steps, the R factor dropped to 0.23 at 8–2.8 Å resolution. During this round of refinement, atomic positional coordinates for the crystallographic dimer were constrained by a strict non-crystallographic twofold axis.

When a cross-rotation function was calculated from human aldehyde reductase using atomic coordinates of porcine aldehyde reductase as the search model and data between 10 and 4 Å resolution with a cut-off radius of 23 Å, one major peak 6.5 standard deviations above background was observed. No other peaks > 70% of this peak were found. Maps of intermolecular vectors were calculated using data between 8 and 4 Å resolution and the molecular translation distance determined. The rotational and translational parameters were refined until a local minimum in the R factor was found. The starting R factor equalled 0.46 and decreased to 0.37 after 11 cycles of refinement using the 2516 reflections between 8 and 4 Å resolution (Fitzgerald, 1988). The refined rotational and translational parameters are: $\alpha = 29.05$, $\beta = 63.93$, $\gamma = 27.4°$, $\delta x = 0.1105$, $\delta y = 0.1285$, and $\delta z = 0.3465$, where α, β, γ are the rotation Euler angles and δx, δy, δz are the translations in fractional coordinates. The initial R factor for the molecular-replacement model equalled 0.36 using 9538 observed reflections out of 11 246 possible unique reflections with a $4.0\sigma(F)$ cut-off for data between 6 and 2.48 Å resolution. Three cycles of rigid-body refinement (Tronrud, Ten Eyck & Matthews, 1987) decreased the R factor to 0.34. The positions of the missing side chains for porcine and human aldehyde reductase were located from $(2F_o - F_c)$ difference maps calculated after the first round of simulated-annealing refinement and were included in the structure-factor calculations for the following cycles of refinement.

Results and discussion

A remarkable feature that exists for the primary sequence of aldose reductase and aldehyde reductase is the high inter-species homology (Fig. 1). Porcine aldose reductase (pALR2) and human aldose reduc-

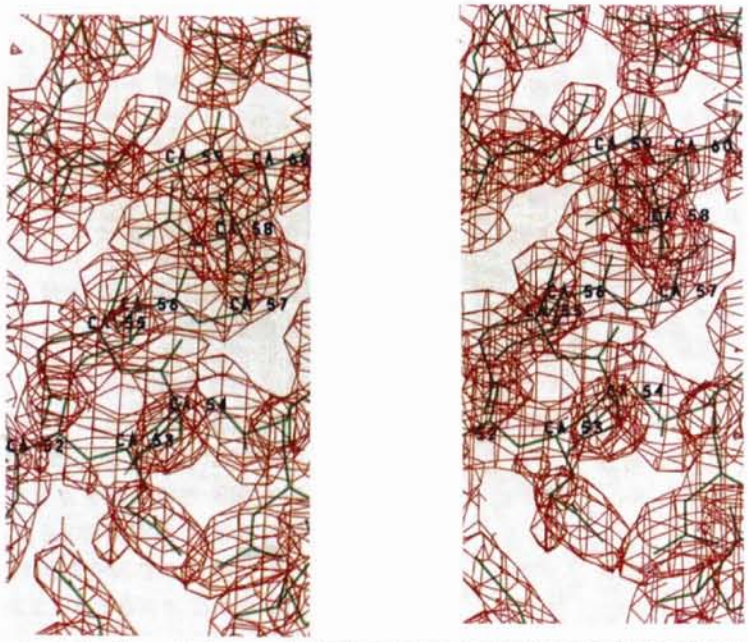

Fig. 2. Stereo drawing showing helix 2 from the human aldehyde reductase model with superimposed electron-density contour surfaces. The 2.48 Å $(2F_o - F_c)$ electron-density map was prepared after simulated-annealing refinement (Brünger *et al.*, 1990). Selected C_α atoms from helix 2 are labeled.

tase (hALR2) exhibit more than 86% sequence identity, and porcine aldehyde reductase (pALR1) and human aldehyde reductase (hALR1) exhibit more than 93% identical residues (Bohren *et al.*, 1989; Kubiseski, Green & Flynn, 1992). The primary sequences of pALR2, hALR2, pALR1 and hALR1 exhibit more than 44% sequence identity.

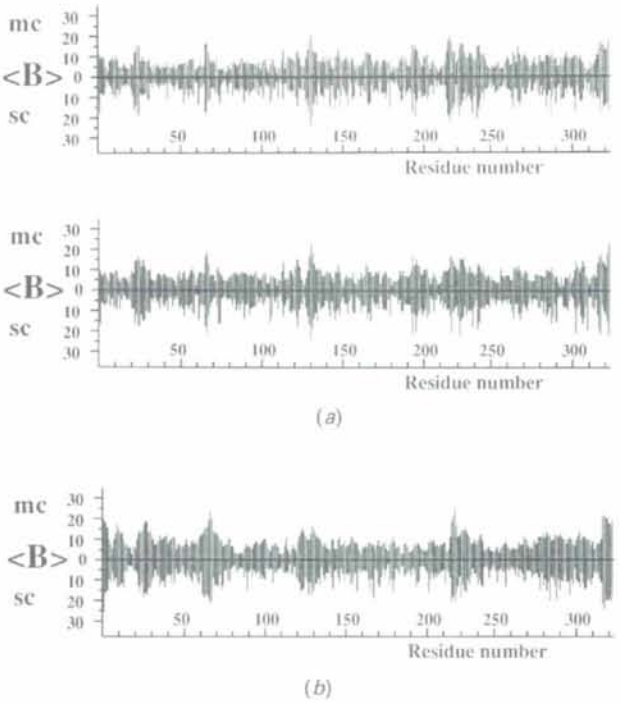

Fig. 3. Average temperature factor (Å^2) per residue, $\langle B \rangle$, computed for main-chain (mc) and side-chain atoms including C_α (sc): (*a*) for the two molecules of porcine aldehyde reductase; (*b*) for the human aldehyde reductase molecule.

The refined models

In the first round of simulated-annealing (SA) refinement for porcine aldehyde reductase (pALR1), the monomers were constrained by the position of the non-crystallographic twofold axis. In the second round, except for the loops and residues at the dimer interface which were declared not equivalent, the refinement was restrained by the position of the non-crystallographic twofold axis. At the end of *X-PLOR* refinement, restrained-parameter least-squares refinement was carried out by using the program *TNT* (Tronrud *et al.*, 1987). The root-mean-square (r.m.s.) shifts of porcine and human aldehyde reductase atomic coordinates at the end of *TNT* refinement were less than 0.01 Å, indicating convergence. The refinement statistics are summarized in Table 1. During the course of the refinement, the crystallographic R factor for porcine aldehyde reductase decreased from 0.40 to 0.19 at 2.8 Å resolution using 85% of the data with a $4.0\sigma(F)$ cut-off. The average uncertainty in the atomic positions for porcine aldehyde reductase calculated from a σ_A plot (Read, 1986) using reflections between 6 and 2.8 Å resolution is 0.32 Å. The starting R factor for human aldehyde reductase using 94% of the data with $4.0\sigma(F)$ cut-off was 0.34 and equalled 0.21 at 2.48 Å resolution after refinement. The quality of the human aldehyde reductase electron-density map after the first round of simulated-annealing refinement revealed that the phases successfully shifted away from the bias of the starting model and allowed for the inclusion of 19 of the missing 20 residues not conserved in porcine and human aldehyde reductase (residue 224 was not located for pALR1 and hALR1 structures). A sample of the human aldehyde reductase electron-density map is shown in Fig. 2. Human

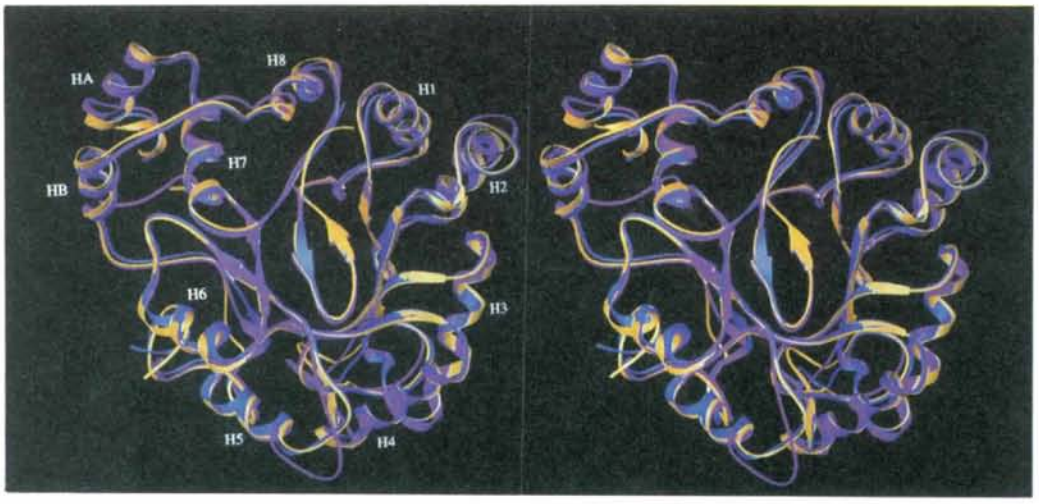

Fig. 4. Stereoview showing the superposition of one molecule from porcine aldehyde reductase (blue), and human aldehyde reductase (yellow), on porcine aldose reductase (magenta). The ten α-helices are labeled according to the nomenclature used.

Table 1. *Refinement statistics for aldehyde reductase*

	pALR1	hALR1
Initial model		
Resolution range (Å)	8.0–2.8	6.0–2.48
No. of reflections	12757	9538
R factor	0.40	0.34
Refitting/*X-PLOR* SA constrained refinement		
Resolution range (Å)	8.0–2.8	
No. of reflections	12757	
R factor	0.23	
Refitting/*X-PLOR* SA restrained refinement		
Resolution range (Å)	6.0 2.8	
No. of reflections	11761	
R factor	0.21	
Refitting/*X-PLOR* SA refinement		
Resolution range (Å)		6.0–2.48
No. of reflections		9538
R factor		0.24
Refitting/*TNT* least-squares refinement		
No. of cycles	30	21
Resolution range (Å)	6.0 2.8	6.0–2.48
No. of reflections	11761	9538
R factor	0.20	0.23
X-PLOR restrained refinement of isotropic temperature factors*		
No. of cycles	12	18
Resolution range (Å)	6.0- 2.8	6.0–2.48
No. of reflections	11761	9538
R factor	0.19	0.21
No. of non-H atoms	4948	2488
R.m.s. deviations from ideal geometry at the end of refinement		
Bond distance (Å)	0.011 (0.020)	0.013 (0.020)
Bond angle (°)	2.5 (3.0)	2.9 (3.0)
Planarity (trigonal) (Å)	0.017 (0.020)	0.015 (0.020)
Planarity (other planes) (Å)	0.018 (0.020)	0.020 (0.020)
Torsion angles† (°)	20.5 (15.0)	19.8 (15.0)

* An isotropic temperature factor of 15.0 Å^2 was used before refinement.

† The torsion angles were not restrained.

Table 2. *Types and positions of amino-acid residues that do not exhibit sequence identity in porcine aldehyde reductase (pALR1) and human aldehyde reductase (hALR1)*

Residue number	pALR1	hALR1	Location
33	Ile	Val	Helix 1
38	Thr	Ser	C-terminal of helix 1
54	Leu	Pro	Helix 2
61	Gln	Lys	Helix 2
63	Thr	Asp	Between helix 2 and strand 3
134	Arg	Cys	Loop *A*
137	Ala	Ser	Loop *A*
142	Asp	Glu	Helix 4
157	Arg	Gln	β-strand 5
165	Ser	Asn	N-terminal of helix 5
172	Val	Ile	Helix 5
224	Asn	Asp	Loop *B*
235	Gln	Leu	Helix *A*
242	Asn	Gly	Between helix *A* and helix 7
265	Val	Ile	Between strand 8 and helix 8
271	Pro	Leu	Helix 8
275	Gln	Lys	Helix 8
290	Asp	Asn	Helix *B*
296	Leu	Trp	Loop *C*
298	Phe	Tyr	Loop *C*

aldehyde reductase atomic coordinates have an average uncertainty of 0.31 Å at 2.48 Å resolution (Read, 1986). In general, there is good correlation between individual isotropic temperature factors and the solvent accessibility for the refined models. Amino-acid residues with the highest temperature factors (Fig. 3) occur at the N-terminus, in a small loop connecting helix 2 and strand 3 (residues 63–74), and in three large exposed loops (residues 115–139, 213–230 and 294–321). No solvent atoms were included in the structure-factor calculations during the refinement process.

Aldehyde reductase folds into an eight-stranded parallel β/α barrel or a triose phosphate isomerase barrel (TIM-barrel) with overall dimensions of approximately $40 \times 40 \times 50$ Å. The aldose and aldehyde reductase structures are completely different from other reductases such as dihydrofolate reductase (Wierenga, Drenth & Schulz, 1983) and glutathione reductase (Karplus & Schulz, 1987) which bind NADPH as a cofactor. The TIM-barrel motif has been observed in approximately two dozen enzymes unrelated in their primary structures, functions, and cofactor requirements (Farber & Petsko, 1990). The core β-strands of aldehyde reductase consist of residues 17–24, 42–48, 75–82, 106–114, 155–163, 181–188, 205–212 and 258–263. The surrounding α-helices consist of residues 28–38, 52–62, 90–102, 140–153, 165–176, 194–203, 245–256 and 266–276.

The symmetrical appearance of the aldehyde reductase molecule is diminished in several ways: (1) the presence of two short antiparallel β-strands at the N-terminus (residues 5–8 and 12–15) connected by a tight turn closing the bottom of the barrel. (2) Three large exposed loops *A*, *B* (at the C-terminal end of β-strands 4 and 7) and *C* (at the C-terminus) partially covering the top of the barrel. (3) Two α-helices: helix *A* between strand 7 and helix 7 (residues 231–241) and helix *B* between helix 8 and loop *C* (residues 286–293). The ten helices and ten β-strands comprise 35 and 22% of the structure, respectively. Out of 20 residues that differ between the primary sequences of porcine and human aldehyde reductase, only residue 157 (Arg in pALR1 and Gln in hALR1) is located in a sheet region (S5). The remaining 19 residues are either located at or close to terminal ends of helices or in loop regions (Table 2) on the surface of the molecule. There are six cysteines in human aldehyde reductase and five cysteines in porcine aldehyde reductase (Cys134 is Arg for the pALR1). No disulfide bridges are present in the structures.

For structural and sequence comparisons, the primary sequences for porcine and human aldose reduc-

tase. and porcine and human aldehyde reductase were aligned and the residue numbering for porcine and human aldehyde reductase used in this study (Fig. 1). The secondary structures of porcine and human aldehyde reductase are highly homologous to porcine aldose reductase. Out of a total of 325 residues, there are two insertions (between residues 178 and 179) and 11 deletions (residues 1, 65, 298, 306–313) in the primary sequences for porcine aldose reductase and human aldose reductase. All of these residues are present on the surface of the molecules and none are part of the secondary structural components or appear to be involved with the critical residues of the cofactor-binding site for the enzymes. The porcine and human aldehyde reductase models include 96% of the amino-acid side chains. The electron density for parts of loop *B* is weak, suggesting high flexibility for this segment. In general, density for the loop regions is better for human aldehyde reductase than for porcine aldehyde reductase structure. This may be a result of the relatively higher resolution data and greater ratio of observable to refinable parameters for human aldehyde reductase compared to porcine aldehyde reductase. In porcine and human aldehyde reductase structures, the positions of residues 218–226 from loop *B* were not determined. Attempts to improve the quality of the electron density in the above-mentioned areas for porcine aldehyde reductase by symmetry-averaging techniques (Furey & Swaminathan, 1990) across the non-crystallographic twofold axis were not successful. Electron density did not exist for the four C-terminal residues of loop *C* (residues 322–325). As a result, these residues were not located and are not included in the refined models.

In human aldose reductase/NADPH structure, upon cofactor binding, loop *B* rotates by 51° around Gly214 and Ser215 (Borhani *et al.*, 1992). This movement allows residues 214–217 to fold over the pyrophosphate and ribose-2′-phosphate portion of NADPH closing off the top of the binding cleft and locking the cofactor in a hydrophobic pocket. In the recombinant human aldose reductase/NADPH structure (Cys300 to Ser mutant) reported by Borhani *et al.* (1992), only broken electron density was seen for residues 218–230 of loop *B* and unambiguous tracing of the main chain was not possible for this segment. Wilson *et al.* (1992) reported loops *A* and *B* to possess highest average temperature factors in the human aldose reductase/NADPH structure. A comparison between human aldose reductase/NADPH and porcine aldose reductase/ADPRP models shows that the additional hydrogen bonding between human aldose reductase and the nicotinamide ring of NADPH (missing in ADPRP) results in the movement of the cofactor away from loop *B*, allowing loop *B* to move over and lock the cofactor into place. On the other hand, ADPRP is not bound to porcine aldose reductase in the exact conformation that NADPH is bound to human aldose reductase, and hence, the pyrophosphate and ribose 2′-phosphate portion of ADPRP hinders closing of loop *B* (Borhani *et al.*, 1992; Rondeau *et al.*, 1992; Wilson *et al.*, 1992).

The main-chain atoms of one molecule from porcine aldehyde reductase and human aldehyde reductase superimpose on the main-chain atoms of porcine aldose reductase structure (same model used in molecular-replacement search) with root-mean-square differences of 1.58 and 1.50 Å, respectively (Fig. 4). In addition, the r.m.s. difference between the main-chain atoms of human aldehyde reductase and the corresponding atoms from porcine aldehyde reductase is 1.04 Å (Brünger *et al.*, 1990). While C_α atoms of the core β-sheet deviate the least among the three structures, C_α atoms that deviate the most (>1.0 Å) belong mainly to residues located in regions on the surface of the molecule (two N-terminal residues; helices 6, 8, *A*, *B*; loops *A*, *B*, *C*) or belong to a segment with residue insertion or deletion in the primary sequence of porcine aldose reductase (between helix 2 and β-strand 3, and between helix 5 and β-strand 6).

Non-crystallographic symmetry

The overall angle of rotation between the refined atomic coordinates for the two non-crystallographic twofold-related molecules of porcine aldehyde reductase is 179.9°. The r.m.s. difference between main-chain atoms and between all atoms for the two molecules equals 0.47 and 0.57 Å, respectively. Intermolecular contacts around the non-crystallographic twofold axis are mainly formed by residues connecting helix 1 with β-strand 2 and helix 2 with β-strand 3 of the α/β barrel from one molecule and their symmetry-related residues from the second molecule (Fig. 5). A main-chain–main-chain hydrogen bond is present between the NH group of Gly40 from the first molecule and the carbonyl O atom of Thr38 from the second molecule. Side-chain–main-chain hydrogen bonding between the two molecules is present between the side chains of Lys34 and Arg42 of the first molecule, and the carbonyl O atoms of Lys68 and Thr38 from the second molecule. The side chain of Glu62 of one molecule is salt linked to the side chain of Lys68 from its non-crystallographic symmetry-related molecule. The side chain of Arg243 (connecting helix *A* with helix 7) from one molecule is hydrogen bonded to the main-chain carbonyl O atom of Asp278 (connecting helix *B* with helix 8) from the second molecule. Except for the salt link between the side chains of Glu62 and Lys68 which occurs in only one direction, all hydrogen-bonding

interactions between the two non-crystallographic symmetry-related molecules obey the non-crystallographic twofold symmetry.

The coenzyme-binding site

The binding sites of NADPH and ADPRP for human and porcine aldose reductase, respectively, have been located (Borhani *et al.*, 1992; Rondeau *et al.*, 1992; Wilson *et al.*, 1992). Attempts are currently underway to co-crystallize complexes of aldehyde reductase/NADPH, aldehyde reductase/NADPH/substrates, and aldehyde reductase/NADPH/inhibitors. NADPH binds human aldose reductase in an unusual extended conformation across the TIM-barrel with the nicotinamide group located in close proximity with a proposed substrate-binding site (Wilson *et al.*, 1992). The conformation of the bound NADPH is more similar to that found for FAD than found in other nicotinamide coenzymes (Borhani *et al.*, 1992). The NADPH-binding site is located at the C-terminal end of the barrel in a large deep elliptical

Fig. 5. The two crystallographically independent molecules for porcine aldehyde reductase with the non-crystallographic twofold axis vertically oriented. The two molecules are viewed down the crystallographic *a* axis. Ribbon drawings were prepared by using the programs described by Carson (1987).

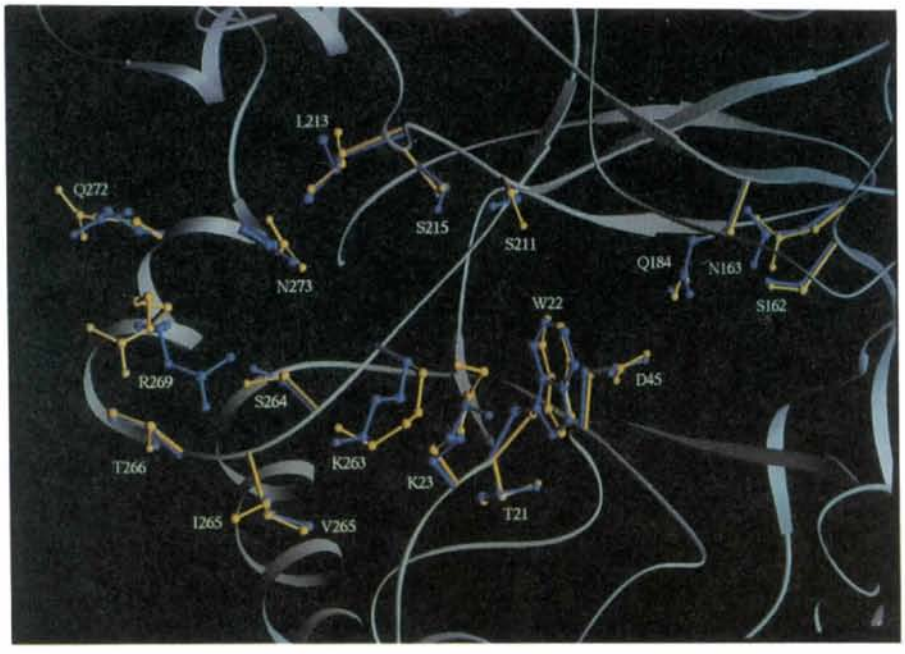

Fig. 6. Superposition of the proposed NADPH-binding residues for porcine aldehyde reductase (blue) and human aldehyde reductase (yellow). Each amino-acid residue is labeled with residue type and number.

Table 3. *Amino-acid residues involved in hydrogen-bonding and salt-linking interactions with NADPH determined from human aldose reductase (hALR2)/NADPH structure (Wilson et al., 1992)*

The residue numbering used is for human aldehyde reductase (hALR1) and porcine aldehyde reductase (pALR1). Amino-acid residues that do not exhibit sequence identity are in upper case.

Residue number	21	22	23	45	162	163	184	211	213	215	263	264	265	266	269	272	273
hALR1	thr	trp	lys	asp	ser	asn	gln	ser	leu	ser	lys	ser	ILE	thr	arg	GLN	asn
pALR1	thr	trp	lys	asp	ser	asn	gln	ser	leu	ser	lys	ser	VAL	thr	arg	GLN	asn
hALR2	thr	trp	lys	asp	ser	asn	gln	ser	leu	ser	lys	ser	VAL	thr	arg	GLU	asn
pALR2	thr	trp	lys	asp	ser	asn	gln	ser	leu	ser	lys	ser	VAL	thr	arg	GLU	asn

cavity bound mainly by the termini of β-strands. NADPH is held in place by 19 hyrodgen bonds and three salt links (Lys23, Lys263 and Arg269). Wilson *et al.* (1992) propose that the 4-*pro-R* hydrogen from the exposed C4 of the nicotinamide of NADPH is transferred to the C atom of the carbonyl group of the substrate and an abstraction of a second H atom from a donor group (possibly Tyr50 or His113) by the negatively charged carbonyl O atom takes place.

Sequence comparisons show most of the critical NADPH-binding residues for human aldose reductase (Wilson *et al.*, 1992) are highly conserved in human and porcine aldehyde reductase, and porcine aldose reductase (Table 3). Out of a total of 17 residues that form hydrogen bonds or salts links with NADPH in the human aldose reductase/NADPH structure, residues 265 and 272 do not exhibit sequence identity in human and porcine aldehyde reductase and human and porcine aldose reductase primary structures. Residue 265 is Ile in human aldehyde reductase instead of Val, and Glu272 in human and porcine aldose reductase is a Gln in human and porcine aldehyde reductase. A superposition of the proposed NADPH-binding residues for human and porcine aldehyde reductase apo-enzymes is shown in Fig. 6.

The main-chain atoms of the proposed cofactor-binding residues from porcine aldehyde reductase superimpose on the corresponding human aldehyde reductase atoms with an r.m.s. difference of 0.35 Å. The r.m.s. difference between all atoms of the proposed cofactor-binding residues from porcine aldehyde reductase, and those from human aldehyde reductase is 0.94 Å (Brünger *et al.*, 1990). Atoms that differ most (>1.0 Å) among the two structures belong to the polar side chains of Lys23, Lys263, Arg269 and Gln272 (residue 272 is a Glu in pALR2 and hALR2). In human aldose reductase, loop *B* rotates by 51° around Gly214 and Ser215 upon binding of NADPH (Borhani *et al.*, 1992). It is possible that side chains of Lys23, Lys263, Arg269 and Gln272 move to form hydrogen bonds or salt links with NADPH upon its binding to the enzyme.

Since the three-dimensional structures of porcine and human aldehyde reductase have been determined without bound cofactor or substrate, it is difficult to predict the exact interactions of aldehyde reductase with cofactor and substrates. However, it is likely that the majority of the residues involved in binding NADPH for aldose reductase will play a critical role in the NADPH-binding site for aldehyde reductase. It is interesting that the cofactor-binding site residues of aldose reductase are highly conserved when taking into consideration that aldose reductase binds NADPH and NADH (with preference to NADPH), while aldehyde reductase binds only NADPH. The structure of human aldose reductase/NADPH was determined without bound substrate (Borhani *et al.*, 1992; Wilson *et al.*, 1992). Wilson *et al.* (1992) predict the substrate-binding site may exist in a region with fewer conserved residues compared to the residues forming the cofactor-binding site. In general, aldehyde reductase prefers aromatic aldehydes as substrates (Markus, Raducha & Harris, 1983). It is possible that the differences in the residues forming the substrate-binding pocket for aldose and aldehyde reductase may be responsible for differences in substrate specificities. In order to clarify the mechanism of action of aldehyde reductase, it will be important to determine the structure of the enzyme complexed with cofactor and a substrate analog. Furthermore, based on the three-dimensional structure information revealed for aldehyde reductase, collaborative arrangements are currently underway to probe structural and functional domains using site-directed mutagenesis to elucidate the mechanism of action for this enzyme.

The structure of aldehyde reductase should be useful in designing specific inhibitors that may be used to alleviate some of the degenerative problems associated with diabetes. Moreover, the high degree of structural homology between aldose and aldehyde reductase may make it possible to design compounds that would inhibit both enzymes by directly binding to their active sites, or may provide insight as to possible non-competitive sites that may be useful targets for drug design.

We thank Dr C. E. Bugg for his support and for reviewing this manuscript. This work was supported by a research grant from the American Diabetes Association (to OEl-K) and from the Medical Research Council of Canada (to TGF). The authors

thank Maxine Rice for preparation of the manuscript.

References

BOHREN, K. M., BULLOCK, B., WERMUTH, B. & GABBAY, K. H. (1989). *J. Biol. Chem.* **264**, 9547–9551.

BORHANI, D. W., HARTER, T. M. & PETRASH, J. M. (1992). *J. Biol. Chem.* **267**, 24841–24847.

BOULTON, A. J. (1986). *Diabetologia*, **29**, 521A.

BRÜNGER, A. T., KRUKOWSKI, A. & ERICKSON, J. (1990). *Acta Cryst.* A**46**, 585–593.

CARSON, M. (1987). *J. Mol. Graphics*, **5**, 103–106.

CROMLISH, J. A. & FLYNN, T. G. (1983). *J. Biol. Chem.* **258**, 3583–3586.

DVORNIK, D., MILLEN, J. & KEMPER, C. (1986). *Diabetes*, **35**(suppl.), 215A.

EATON, R. P., SIBBITT, W. L. & HARSH, A. (1985). *J. Am. Med. Assoc.* **253**, 1437–1440.

EL-KABBANI, O., LIN, G., NARAYANA, S. V. L., MOORE, K. M., GREEN, N. C., FLYNN, T. G. & DELUCAS, L. J. (1993). *Acta Cryst.* D**49**, 490–496.

EL-KABBANI, O., NARAYANA, S. V. L., BABU, Y. S., MOORE, K. M., FLYNN, T. G., PETRASH, J. M., WESTBROOK, E. M., DELUCAS, L. J. & BUGG, C. E. (1991). *J. Mol. Biol.* **218**, 695–398.

FARBER, G. K. & PETSKO, G. A. (1990). *Trends Biol. Sci.* **15**, 228–234.

FITZGERALD, P. M. D. (1988). *J. Appl. Cryst.* **21**, 273–278.

FLYNN, T. G. (1982). *Biochem. Pharmacol.* **31**, 2705–2712.

FRANK, R. N., KEIRN, R. J., KENNEDY, A. & FRANK, W. K. (1983). *Invest. Ophthalmol. Vis. Sci.* **24**, 1519–1529.

FUREY, W. & SWAMINATHAN, S. (1990). Am. Crystallogr. Assoc. Meet. p. 73, Abstract 18.

GONZALEZ, R. G., BARNETT, P., AGUAYO, J., CHEN, H. M. & CHYLACK, L. T. JR (1984). *Diabetes*, **33**, 196–199.

HOWARD, A. J., GILLIAND, G. L., FINZEL, B. C., POULOS, T L., OHLENDORF, D. H. & SALEMME, F. R. (1987). *J. Appl. Cryst.* **20**, 382–387.

JONES, A. T. (1978). *J. Appl. Cryst.* **11**, 268–272.

KADOR, P. R. & KINOSHITA, J. H. (1984). *Ciba Found. Symp.* **106**, 110–131. London: Pitmann.

KARPLUS, P. A. & SCHULZ, G. E. (1987). *J. Mol. Biol.* **195**, 701–729.

KINOSHITA, J. H. (1974). *Invest. Ophthalmol.* **13**, 713–724.

KINOSHITA, J. H., KADOR, P., ROBINSON, W. G. (1984). *Ann. Intern. Med.* **101**, 82–91.

KINOSHITA, J. H. & NISHIMURA, C. (1988). *Diabetes Metab. Rev.* **4**, 323–337.

KOJIMA, K., MATSUBARA, H., HARADA, T., MIZUMO, K., SUZUKI, M., NIGISHI, H., HIRONUBU, K. & SAKAMOTO, N. (1985). *Jpn. J. Ophthalmol.* **29**, 99–109.

KUBISESKI, T. J., GREEN, N. C. & FLYNN, T. G. (1992). *Enzymology and Molecular Biology of Carbonyl Metabolism*, edited by H. WEINER, T. G. FLYNN & D. W. CRABB, p. 4. New York: Plenum Press.

MCPHERSON, A. (1985). *Methods Enzymol.* **114**, 112–120.

MARKUS, H. B., RADUCHA, M. & HARRIS, H. (1983). *Biochem. Med.* **29**, 31–45.

READ, R. (1986). *Acta Cryst.* A**42**, 140–149.

ROBINSON, W. G., KADOR, P. F., AKAGI, Y., KINOSHITA, J. H., GONZALEZ, R. & DVORNIK, D. (1986). *Diabetes*, **35**, 295–299.

ROBINSON, W. G., KADOR, P. F. & KINOSHITA, J. H. (1983). *Science*, **221**, 1177–1179.

RONDEAU, J.-M., TÊTE-FAVIER, F., PODJARNY, A., REYMANN, J.-M., BARTH, P., BIELLMANN, J. F. & MORAS, D. (1992). *Nature (London)*, **355**, 469–472.

RYDER, S. (1986). *Diabetologia*, **29**, 588A.

SAMBROOK, J., FRITSCH, E. F. & MANIATIS, T. (1990). *Molecular Cloning A Laboratory Manual*, 2nd ed. Cold Spring Harbour Press.

SHANKS, E., D'AMICO, D. J. & GRAGOUDAS, E. S. (1985). *Invest. Ophthalmol. Vis. Sci.* **26**(Suppl.), 28.

SIAKI, R. K., SCHARF, S., GALOONA, F., MULLIS, K. B., HORN, G. T., ERLICH, H. A. & ARNHEIM, N. (1985). *Science*, **230**, 1350–1354.

SPIELBERG, S. P., SHEAR, N. H., CANNON, M., HUTSON, N. J. & GUNDERSON, K. (1991). *Ann. Intern. Med.* **114**, 720–724.

SRIVASTAVA, S. K., PETRASH, J. M., SADANA, I. J., ANSARI, N. H. & PARTRIDGE, C. A. (1982). *Curr. Eye Res.* **2**, 407–410.

TOMLINSON, D. R. & MAYER, J. H. (1984). *J. Auton. Pharmacol.* **4**, 59–72.

TRONRUD, D. E., TEN EYCK, L. F. & MATHEWS, B. W. (1987). *Acta Cryst.* A**43**, 498–501.

WARD, J. D. (1985). *The Diabetes Annual.* 1, edited by K. ALBERTI & L. P. KRALL, pp. 288–308. Amsterdam, New York, Oxford: Elsevier.

WIERENGA, R. K., DRENTH, J. & SCHULS, G. E. (1983). *J. Mol. Biol.* **167**, 725–739.

WILLIAMSON, J. R., CHANG, K., ROWOLD, E., MARVEL, J., TOMLINSON, M., SHERMAN, W. R., ACKERMANN, K. E. & KILO, C. (1985). *Diabetes*, **34**, 703–705.

WILSON, D. K., BOHREN, K. M., GABBAY, K. H. & QUIOCHO, F. A. (1992). *Science*, **257**, 81–84.